Inorganica Chimica Acta, *197* (1992) 141–147

Syntheses and characterization of binuclear manganese(III,IV) and (IV,IV) complexes with 1,4,7,10-tetraazacyclododecane (cyclen)

Patricia A. Goodson, Derek J. Hodgson
Department of Chemistry, University of Wyoming, Laramie, WY 82071 (USA)

Jørgen Glerup, Kirsten Michelsen and Høgni Weihe
Chemistry Laboratory I, H.C. Ørsted Institute, Universitetsparken 5, DK-2100 Copenhagen Ø (Denmark)

(Received February 19, 1992)

Abstract

The synthesis and characterization of di-μ-oxodimanganese(III,IV) and (IV,IV) complexes employing the tetradentate ligand 1,4,7,10-tetraazacyclododecane (cyclen) are reported. The crystal structure of the Mn(III,IV) complex, di-μ-oxo-bis(1,4,7,10-tetraazacyclododecane)dimanganese(III,IV) chloride lithium chloride pentahydrate, $[(\text{cyclen})\text{Mn(III)O}_2\text{Mn(IV)}(\text{cyclen})]\text{Cl}_3\cdot\text{LiCl}\cdot5\text{H}_2\text{O}$ (**1a**), has been established by three dimensional X-ray diffraction techniques. The complex, of formula $\text{Mn}_2\text{C}_{16}\text{H}_{50}\text{N}_8\text{O}_7\text{Cl}_4\text{Li}$, crystallizes in the monoclinic space group *C*2/*c* with four molecules in a cell of dimensions $a=20.284(4)$, $b=10.576(2)$, $c=15.345(2)$ Å and $\beta=105.70(1)°$. The structure was solved by direct methods and refined by least-squares techniques to a final agreement factor of 0.0344 based on 3445 observed independent intensities. The dimer has a crystallographic inversion center in the middle, which is due to a static disorder in the crystals. The Mn–Mn distance in the complex is 2.694(1) Å and the bridging Mn–O–Mn angle is 95.7(1)°. The magnetic properties of the III/IV complex are consistent with a doublet ground state, the observed J value of $-138(2)$ cm^{-1} for **1a** and $-156.5(5)$ cm^{-1} for the corresponding perchlorate salt being similar to those observed in other III/IV complexes. The Mn(IV,IV) complex has a singlet ground state, with $J=-144.5(10)$ cm^{-1}. The EPR spectrum of the III/IV complex exhibits the commonly-occurring sixteen line pattern, with a significant degree of anisotropy. The EPR spectrum has been simulated by diagonalization of the energy matrix for the doublet state. The complex exhibits two quasi-reversible waves in the cyclic voltammogram, with redox potentials of 0.069 and 0.846 V (versus Ag/AgCl) for the III/III↔III/IV and III/IV↔IV/IV couples, respectively. The electronic spectra of both the (III,IV) and (IV,IV) forms of the complex are similar to those of analogous complexes.

Introduction

We and others continue to pursue the synthesis and chemical and physical properties of bridged binuclear manganese complexes, both because of the role of binuclear and polynuclear manganese species in biological systems and because of their potential use as redox catalysts. Following the successful isolation of the 2,2′-bipyridine (bpy) [1] and 1,10-phenanthroline (phen) [2] complexes of the types $[\text{L}_2\text{MnO}]_2^{3+/4+}$, a wide variety of other di-μ-oxodimanganese dimers incorporating tetradentate ligands in place of the bidentate bpy and phen have been synthesized [3–17]; the use of tetradentate ligands is expected to reduce the labilities of the various binuclear species which are involved in the (IV/IV)↔(III/IV) and (III/IV)↔(III/III) couples and hence to facilitate the use of these complexes in electrocatalytic cycles. In recent publications, the isolation of all three redox states, Mn(III,III) [5, 9], Mn(III,IV) [1–4, 6–8, 10–14, 17] and Mn(IV/IV) [2, 6, 8, 14–17] has been reported, although to date no single system has been obtained in which all three forms have been isolated.

Based on the success of our earlier work on analogous dimeric chromium(III) complexes and on monomeric manganese systems [18, 19] we chose to investigate the use of the tetradentate ligands 1,4,8,11-tetraazacyclotetradecane (cyclam) and 1,4,7,10-tetraazacyclododecane (cyclen) in the synthesis of manganese dimers of this general type. We have previously reported the results of our work with cyclam [7], and Brewer *et al.* have reported the synthesis and characterization of Mn(III,IV) complexes with both ligands [11, 13]. We have now obtained more complete data on both the (III,IV) and the (IV,IV) cyclen species, and we report the results of our investigations here.

0020-1693/92/$5.00

Experimental

Syntheses

The hydrochloride salt of the ligand, 1,4,7,10-tetraazacyclododecane hydrochloride [cyclen·4HCl] was prepared by the method of Richman and Atkins [20].

Di-μ-oxo-bis(1,4,7,10-tetraazacyclododecane)-dimanganese(III,IV) chloride lithium chloride pentahydrate, [(cyclen)Mn(III)O_2Mn(IV)(cyclen)]Cl_3·LiCl·$5H_2O$ (1a)

Cyclen·4 HCl (0.318 g, 1.00 mmol) was dissolved in an aqueous solution of lithium hydroxide (2 ml, 2 M). Ethanol (8 ml, 96%) was added followed by $MnCl_2\cdot 4H_2O$ (0.197 g, 1.00 mmol). Air was bubbled through the solution, until the solution was dark green, and a filtered solution of LiCl in ethanol (approx. 0.20 g in 5 ml) was added. The solvent was allowed to slowly evaporate. After filtering off the first crop of large, glistening, green crystals (0.122 g) and washing with ethanol (96%), a small amount of water was added to the mixed filtrate and washing liquid in order to avoid precipitation of lithium chloride. The solution was further evaporated to give another crop of 0.110 g. Total yield 64%. *Anal.* Calc. for $[Mn(C_8H_{20}N_4)O]_2Cl_3\cdot LiCl\cdot 5H_2O$: Mn, 15.15; C, 26.50; N, 15.45; H, 6.94; Cl, 19.55. Found: Mn, 15.16; C, 26.29; N, 15.51; H, 7.23; Cl, 19.97%.

Di-μ-oxo-bis(1,4,7,10-tetraazacyclododecane)-dimanganese(III,IV) nitrate, [(cyclen)Mn(III)O_2Mn(IV)(cyclen)]$(NO_3)_3$ (1b)

A dark-green ethanolic solution was obtained as described above, but from $Mn(NO_3)_2\cdot 6H_2O$ (0.278 g, 1.00 mmol). The solution was evaporated to a moist mass, and the residue was then treated with acetone. The green powder was filtered and washed with acetone. Yield 0.461 g (60%). *Anal.* Calc. for $[Mn(C_8H_{20}N_4)O]_2(NO_3)_3$: Mn, 16.63; C, 28.58; N, 22.99; H, 6.00. Found: Mn, 16.57; C, 28:80; N, 21.61; H, 6.09%. The slightly impure compound was used as a starting material for the synthesis of the perchlorate salt.

Di-μ-oxo-bis(1,4,7,10-tetraazacyclododecane)-dimanganese(III,IV) perchlorate dihydrate, [(cyclen)Mn(III)O_2Mn(IV)(cyclen)]$(ClO_4)_3$·$2H_2O$ (1c)

$[Mn(cyclen)O]_2(NO_3)_3$ (0.450 g, c. 0.67 mmol) was extracted on a filter with water (3 ml). The solution was added dropwise to a solution of sodium perchlorate (3 g) in water (3 ml). Cooling on ice resulted in the precipitation of small bluish-green crystals. These were washed with an aqueous solution of sodium perchlorate (1 M) and with ethanol (96%). Yield 0.115 g (21%). Recrystallization from water reduced the yield by 50%. *Anal.* Calc. for $[Mn(C_8H_{20}N_4)O]_2(ClO_4)_3\cdot 2H_2O$: C, 23.41; N, 13,65; H, 5.40; Cl, 12.96. Found: C, 23.29; N, 13.73; H, 4.95; Cl, 13.40%. In other cases the compound crystallized with 4 moles of water. The absorption spectrum was identical with the spectrum for the chloride.

Di-μ-oxo-bis(1,4,7,10-tetraazacyclododecane)-dimanganese(IV) chloride perchlorate dihydrate, [(cyclen)Mn(IV)O_2Mn(IV)(cyclen)]Cl$(ClO_4)_3$·$2H_2O$ (2)

$[Mn(cyclen)O]_2Cl_3\cdot LiCl\cdot 5H_2O$ (0.200 g, 0.276 mmol) was dissolved in water (4 ml). The solution was cooled on ice, and the same volume of a solution of perchloric acid (1 M) was added. After 1 h the olive-green crystals were filtered and washed with a solution of sodium perchlorate (1 M) and with ethanol (96%). Yield 0.063 g (27%). *Anal.* Calc. for $[Mn(C_8H_{20}N_4)O]_2Cl(ClO_4)_3\cdot 2H_2O$: Mn, 12.83; C, 22.44; N, 13.09; H, 5.18; Cl (total), 16.56; Cl, (ionic), 4.14. Found: Mn, 12.95; C, 22.50; N, 13.17; H, 5.22; Cl (total), 16.70; Cl (ionic), 4.62%. In other cases the compound crystallized with 1 mol of water.

Spectroscopy

Electronic absorption spectra were recorded on a Perkin-Elmer Lambda 17 spectrometer. The solvents were chosen so as to maximize the stability of each complex. EPR spectra were recorded at liquid helium temperature on a Bruker ESP 300 spectrometer operating at a frequency of 9.38 GHz (X-band) with magnetic field modulation of 100 kHz, modulation amplitude of 7 G, and microwave power of 10 mW. Samples were examined as frozen glasses in *N*-methylformamide solution.

Magnetochemistry

Magnetic susceptibilities of powdered samples were measured by the Faraday method in the temperature range 2–300 K at a field strength of 1.3 T. The magnetic field was calibrated with $Hg[Co(NCS)_4]$ [21]. A detailed description of the instrumentation has been published elsewhere [22, 23]. The molar susceptibilities were corrected for ligand diamagnetism using Pascal's constants.

Electrochemistry

Cyclic voltammetry was performed on a BAS-100A electrochemical analyzer using a glassy carbon working electrode and a platinum auxiliary electrode. Voltages are reported relative to Ag/AgCl. Solutions were 2×10^{-3} M in manganese complex in acetonitrile with 0.1 M tetrabutylammonium perchlorate as supporting electrolyte.

X-ray crystallography

The crystal structure of complex **1a** was determined at 23 °C on a Nicolet R3m/V diffractometer equipped with a molybdenum tube ($\lambda K\alpha_1 = 0.70926$ Å; $\lambda K\alpha_2 = 0.71354$ Å) and a graphite monochromator. Experimental details and cell constants are collected in Table 1. The structure was solved by direct methods and refined by full-matrix least-squares techniques. The programs used were from the SHELXTL system [24]. Hydrogen atoms were placed in calculated positions (C–H = 0.96 Å), while other atoms were refined anisotropically. Final values of the agreement factors are $R = 0.0344$, $R_w = 0.0541$ based on 3445 independent intensities with $I \geqslant 3\sigma(I)$. The positional parameters of the non-hydrogen atoms are presented in Table 2. See also 'Supplementary material'.

Results and discussion

Mn(III,IV) complexes

Structure of the Mn(III,IV) complex (1a)

The crystals contain apparently centrosymmetric binuclear $[(\text{cyclen})\text{MnO}]_2^{3+}$ cations, lithium cations, chloride anions, and water molecules which are linked by hydrogen bonds. A view of the binuclear cation is given in Fig. 1, and principal bond lengths and angles are provided in Tables 3 and 4, respectively.

The geometry about each manganese center is roughly octahedral, the ligating atoms being two *cis* oxo bridges and the four nitrogen atoms from the cyclen ligand. The presence of a crystallographic inversion center in the middle of the dimer causes the two manganese

TABLE 1. Crystallographic and data collection parameters for **1a**

Formula	$Mn_2C_{16}H_{50}N_8O_7Cl_4Li$
Color	dark green
System	monoclinic
Space group	*C*2/*c*
Cell dimensions	
a (Å)	20.284(4)
b (Å)	10.576(2)
c (Å)	15.345(2)
β (°)	105.70(1)
Volume (Å³)	3169(1)
Z	4
F(000)	1476
T (°C)	23.0
Absorption coefficient (mm⁻¹)	1.15
Index ranges	$0 \leqslant h \leqslant 28$
	$0 \leqslant k \leqslant 14$
	$-21 \leqslant l \leqslant 21$
No. reflections	4630
Observed independent reflections	3445 ($F \geqslant 6\sigma(F)$)
R	0.0344
R_w	0.0541

TABLE 2. Atomic coordinates ($\times 10^4$) and equivalent isotropic displacement coefficients ($Å^2 \times 10^3$)

	x	*y*	*z*	U_{eq} [a]
Mn(1)	2041(1)	1772(1)	5258(1)	19(1)
O(1)	2158(1)	2412(1)	4215(1)	27(1)
N(1)	1130(1)	897(2)	4540(1)	26(1)
N(4)	2422(1)	−149(2)	5247(1)	30(1)
N(7)	1991(1)	1114(2)	6519(1)	24(1)
N(10)	1323(1)	3104(2)	5561(1)	31(1)
C(2)	1184(1)	−487(2)	4641(2)	32(1)
C(3)	1892(1)	−865(2)	4570(2)	36(1)
C(5)	2577(1)	−698(2)	6182(2)	33(1)
C(6)	2607(1)	346(2)	6870(1)	30(1)
C(8)	1928(1)	2254(2)	7049(1)	32(1)
C(9)	1299(1)	2947(2)	6519(2)	35(1)
C(11)	656(1)	2884(3)	4881(2)	40(1)
C(12)	528(1)	1480(3)	4765(2)	37(1)
Cl(1)	974(1)	593(1)	2269(1)	40(1)
Cl(2)	1302(1)	−3852(1)	5450(1)	44(1)
Li	0	−4702(6)	7500	39(2)
O(1W)	0	1598(3)	7500	50(1)
O(2W)	598(1)	−3573(2)	7066(1)	50(1)
O(3W)	452(1)	−6011(2)	8392(2)	60(1)

[a] Equivalent isotropic *U* defined as one third of the trace of the orthogonalized U_{ij} tensor.

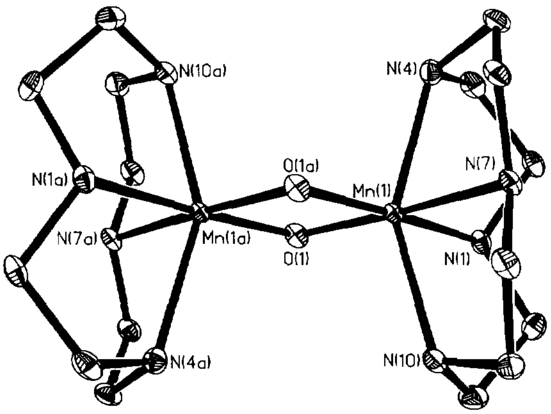

Fig. 1. View of the cation in the Mn(III,IV) complex **1a**. Unlabelled atoms are carbon atoms, and hydrogen atoms are omitted for clarity.

TABLE 3. Bond lengths (Å)

Mn(1)–O(1)	1.812(2)	Mn(1)–N(1)	2.094(2)
Mn(1)–N(4)	2.175(2)	Mn(1)–N(7)	2.085(2)
Mn(1)–N(10)	2.166(2)	Mn(1)–Mn(1A)	2.694(1)
Mn(1)–O(1A)	1.823(1)	N(1)–C(2)	1.473(3)
N(1)–C(12)	1.489(3)	N(4)–C(3)	1.485(3)
N(4)–C(5)	1.501(3)	N(7)–C(6)	1.465(3)
N(7)–C(8)	1.479(3)	N(10)–C(9)	1.492(3)
N(10)–C(11)	1.486(3)	C(2)–C(3)	1.521(4)
C(5)–C(6)	1.518(3)	C(8)–C(9)	1.505(3)
C(11)–C(12)	1.510(4)	Li–O(2W)	1.944(4)
Li–O(3W)	1.988(5)		

TABLE 4. Bond angles (°)

O(1)–Mn(1)–N(1)	90.5(1)	O(1)–Mn(1)–N(4)	102.1(1)
N(1)–Mn(1)–N(4)	81.3(1)	O(1)–Mn(1)–N(7)	174.8(1)
N(1)–Mn(1)–N(7)	94.8(1)	N(4)–Mn(1)–N(7)	78.6(1)
O(1)–Mn(1)–N(10)	101.7(1)	N(1)–Mn(1)–N(10)	81.4(1)
N(4)–Mn(1)–N(10)	150.5(1)	N(7)–Mn(1)–N(10)	79.2(1)
O(1)–Mn(1)–O(1A)	84.3(1)	N(1)–Mn(1)–O(1A)	174.8(1)
N(4)–Mn(1)–O(1A)	99.8(1)	N(7)–Mn(1)–O(1A)	90.4(1)
N(10)–Mn(1)–O(1A)	99.6(1)	Mn(1)–O(1)–Mn(1A)	95.7(1)
Mn(1)–N(1)–C(2)	110.7(1)	Mn(1)–N(1)–C(12)	111.0(1)
C(2)–N(1)–C(12)	115.4(2)	Mn(1)–N(4)–C(3)	106.8(1)
Mn(1)–N(4)–C(5)	109.7(1)	C(3)–N(4)–C(5)	113.3(2)
Mn(1)–N(7)–C(6)	106.0(1)	Mn(1)–N(7)–C(8)	105.7(1)
C(6)–N(7)–C(8)	116.2(2)	Mn(1)–N(10)–C(9)	110.0(1)
Mn(1)–N(10)–C(11)	106.6(2)	C(9)–N(10)–C(11)	114.1(2)
N(1)–C(2)–C(3)	107.4(2)	N(4)–C(3)–C(2)	109.6(2)
N(4)–C(5)–C(6)	110.0(2)	N(7)–C(6)–C(5)	106.1(2)
N(7)–C(8)–C(9)	106.6(2)	N(10)–C(9)–C(8)	109.7(2)
N(10)–C(11)–C(12)	109.4(2)	N(1)–C(12)–C(11)	108.0(2)
O(2W)–Li–O(3W)	116.7(1)	O(2W)–Li–O(2WA)	104.2(3)
O(2W)–Li–O(3WA)	113.9(1)	O(3W)–Li–O(3WA)	91.7(3)

centers to be crystallographically equivalent. This effect, which has been observed in several other Mn(III,IV) dimers of this type [2b, 7, 8], can be attributed to a static disorder in the crystals. Thus, the average axial Mn–N bond length of 2.170(6) Å is longer than the average equatorial bond length of 2.090(6) Å, as expected for a d^4 Mn(III) center but not for a d^3 Mn(IV) center. The observed difference of 0.080 Å is the same as that of 0.081 Å observed in the statically disordered bromide salt of the cyclam complex [7], but is much smaller than the value of 0.226 Å found by Brewer *et al.* at the Mn(III) site in the ordered triflate salt of the cyclam complex [13]. The average Mn–O distance of 1.818(8) Å compares well with the value 1.821(1) in the cyclam bromide [7]; this value is intermediate between the values of 1.862(9) and 1.788(3) Å for the Mn(III)–O and Mn(IV)–O bonds, respectively, in the triflate. It is, however, noteworthy that the present average is similar to the value of 1.825 Å which is the average of the Mn(III)–O and Mn(IV)–O bond lengths in the triflate salt [13].

The contraction of the chelate ring size on going from the cyclam ligand to cyclen might be expected to affect the geometry of the complex. In fact, the Mn–Mn separation of 2.694(1) Å in the cyclen complex is shorter than the value of 2.731(2) Å in the bromide salt of the cyclam complex [7], but is within the range of 2.64–2.74 Å found in other Mn(III,IV) dimers of this type. The Mn–O–Mn bond angle of 95.7(1)° and the *trans* N–Mn–N angle of 150.5(1)° are also slightly smaller than the respective values of 97.2(1) and 158.6(2)° found for the corresponding angles in the bromide salt of the cyclam(III,IV) complex [7].

As was noted above, the crystals contain one Li$^+$ cation, four Cl$^-$ anions, and five water molecules per binuclear cation. The Li$^+$ cation is tetrahedrally surrounded by oxygen atoms O(2W), O(3W), O(2WA) and O(3WA) from four separate water molecules. The Li–O distances range from 1.944 to 1.988 Å (av. 1.966(25) Å) and the O–Li–O angles range from 91.7 to 116.7° (av. 109.5(1.0)°).

Electrochemistry

The cyclic voltammogram of the perchlorate salt (**1c**) shows two quasi-reversible redox couples at 0.069 and 0.846 V versus Ag/AgCl. The lower potential wave, which corresponds to the one-electron process Mn(III,IV) ↔ Mn(III,III), can be compared to the value of 0.195 V reported by Brewer *et al.* [11]*. The higher potential wave, corresponding to the Mn(III,IV) ↔ Mn(IV,IV) couple, can be compared to the value of 0.945 V reported by Brewer *et al.* [11]*. The present values are also comparable to the values reported for the cyclam complex, but are significantly lower than those we have reported for a variety of systems containing aromatic nitrogen-containing ligands [6, 8, 17].

Spectroscopy

The electronic spectra of the Mn(III,IV) complex (**1a**) in two different solvents are compared with that of the Mn(IV,IV) complex (**2**) in Table 5, and the visible region of the spectrum of the (III,IV) complex is shown in Fig. 2. The spectrum consists of two intense maxima in the UV region (at 381 and 430 nm) and three bands of medium intensity in the visible region (at 554, 658 and 696 nm). This spectrum is consistent with those reported for a variety of Mn(III,IV) analogues [6].

TABLE 5. Absorption spectra of dimeric complexes of manganese(III) and (IV) with cyclen

Compound	Solvent	$\lambda(\epsilon)$
1a	water	696(666), 658(676), 554(535), 430(sh 1275), 381(1741)
	N-methylformamide	697(667), 652(678), 554(550), 430(sh 1289), 379(1769)
2	0.1 M HClO$_4$	780(sh 308), 710(sh 874), 664(1186), 529(564), 450(sh 1539), 390(5405)

---

*The value of 0.195 V vs. Ag/AgCl was calculated from the value of −0.20 V vs. Ag/Ag+ by applying the corrections of E(SCE) = E(Ag/Ag+) + 0.35 V (see ref. 13), E(Ag/AgCl) = E(SCE) + 0.045 (see ref. 25).

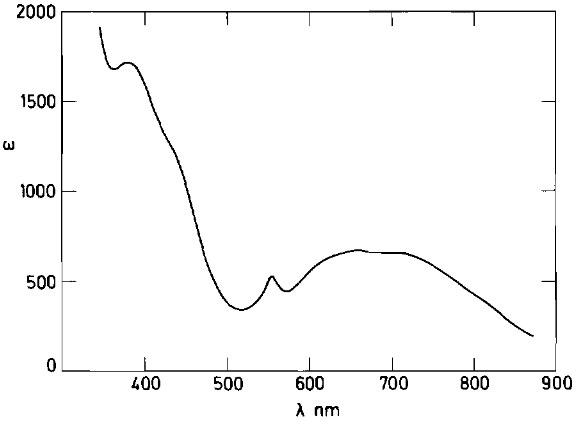

Fig. 2. The electronic absorption spectrum of the Mn(III,IV) complex **1a** in water.

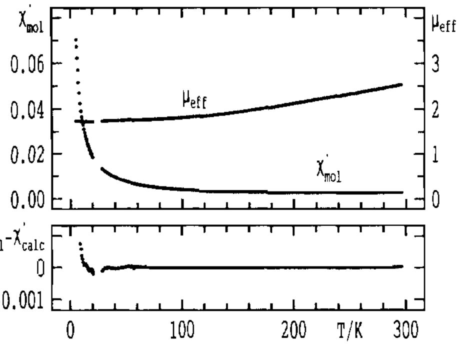

Fig. 3. The magnetic susceptibility (left scale) and effective magnetic moment (right scale) of the Mn(III,IV) complex **1c**. The lower curve shows the fit to the values calculated from the theoretical expression (see text) using the parameters $g_1 = g_2 = 1.94$, $2J = -313$ cm^{-1}.

Magnetic susceptibility

The temperature dependence of the magnetic susceptibility of powdered samples of the mixed-valent (III,IV) complexes **1a** and **1c** was measured in the range 2–300 K; the magnetic properties of the two complexes are substantially similar, and the data for complex **1c** are presented in Fig. 3. As is shown in Fig. 3, the effective magnetic moment declines monotonically from a room temperature value of approximately 2.45 μ_B to a value of 1.7 μ_B at 20 K; the moment appears to increase slightly below 20 K. The value of 1.7 μ_B is that expected for the spin only moment of a complex with a doublet ground state.

The temperature dependence of the magnetic susceptibility $X'_{\mathrm{mol,exp}}$ was approximated within the framework of non-linear regression analysis using the expressions we have defined elsewhere [17]. The energies E_i of the twenty components of the ground state manifold were obtained using an isotropic spin Hamiltonian operator [17] where we have assumed that the g values for the two manganese atoms are identical. The Heisenberg term $-2JS_1 \cdot S_2$ gives energies of the quartet, sextet, and octet states of $-3J$, $-8J$ and $-15J$, respectively, relative to the doublet ground state. For complex **1a**, the fitting leads to values of $g_1 = g_2 = 1.93 \pm 0.02$, $2J = -275 \pm 4$ cm^{-1}, $J = -138 \pm 2$ cm^{-2}, while for **1c** the corresponding values are $g_1 = g_2 = 1.94 \pm 0.01$, $2J = -313 \pm 1$ cm^{-1}, $J = -156.5 \pm 0.5$ cm^{-1}. These values of J can be compared to those of -118 to -272 cm^{-1} reported for other mixed-valent di-μ-oxodimanganese(III,IV) complexes [2b, 6–8, 10, 12, 17, 26]. It is noteworthy that the magnitude of $2J$ observed here for the cyclen complexes is greater than that found for the bromide salt of the cyclam complex ($2J = -237$ cm^{-1}) while the bridging Mn–O–Mn angle in the cyclen complex **1a** is smaller than that in the cyclam complex. This apparent trend, which is also discernible from the data summarized by Libby *et al.* [16] is opposite to that observed in related binuclear systems of copper(II) and chromium(III) [27, 28].

EPR spectra

The EPR spectrum of the (III,IV) complex **1a** is presented in Fig. 4 and shows the familiar sixteen line pattern [6, 8, 17, 26]. The spectrum shows significant anisotropy, as seen previously for several other complexes. The spectrum of the complex was computer simulated in order to increase our understanding of the anisotropy. The energy matrix for the doublet state ($S = 1/2$), which has the dimensions 72×72, was generated for each orientation of the magnetic field relative to the molecular z axis. The energy matrix was calculated by means of the spin Hamiltonian operator

$$\mathcal{H} = g_1 \mu_B \hat{S}_1 \cdot \hat{H} + g_2 \mu_B \hat{S}_2 \cdot \hat{H} + A_1 \hat{S}_1 \cdot \hat{I}_1 + A_2 \hat{S}_2 \cdot \hat{I}_2$$

with $S_1 = 2$ and $S_2 = 3/2$.

The resonance condition for each transition was found by successive diagonalizations and iterations, and the relative intensity was calculated from the eigenvectors. Summation of all the transitions over all space gives

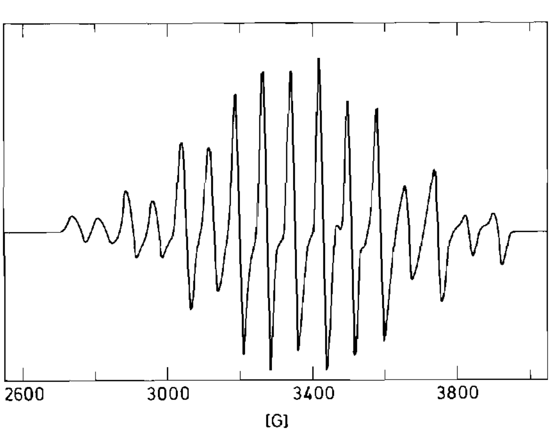

Fig. 4. The EPR spectrum (79 K) of the Mn(III,IV) complex **1a**.

the simulated spectrum; the programs developed for the simulation have been described elsewhere [17, 29, 30]. Diagonalization of the energy matrix instead of the more usual perturbation treatment [26], which neglects the non-diagonal elements of the energy matrix, gives a more reliable simulation but is much more time consuming.

The simulated spectrum shown in Fig. 5 was calculated with the parameter values $A_{1x}=-0.0075$, $A_{1y}=-0.0072$, $A_{1z}=-0.0063$, $A_{2x}=-0.0073$, $A_{2y}=-0.0071$, $A_{2z}=-0.0068$ cm^{-1}; $g_{1x}=2.000$, $g_{1y}=1.988$, $g_{1z}=1.997$, $g_{2x}=g_{2y}=g_{2z}=1.994$. The parameters were obtained by a trial and error process, but since it is almost impossible to determine twelve independent parameters in this way it was assumed that the parameters for the Mn(IV) ion are more nearly isotropic than those for the Mn(III) ion. The upper graph gives the resonance condition for the 36 allowed transitions as a function of the orientation of the magnetic field relative to the coordinate system. Since the measurement was not performed on a single crystal, we are unable to relate the crystallographic coordinate system to the coordinate system used in the computer simulation.

The simulation process allows us to comment on the observed structure in the EPR spectrum. The first line, observed near 2750 G, is structured because the line in the *xz* plane has a slightly lower energy than that in the *yz* plane, while the transition with the field parallel to the *z* axis occurs near 2810 G. For the line observed around 3910 G, the components in the *xz* and *yz* planes are closer together, while the shoulder observed around 3875 G is the *z* component. The lower part of Fig. 5 shows the simulated spectrum. As a model for the individual lines we have used a differentiated gaussian line shape with a halfwidth of 24 G. In other publications [26] on the simulation of this kind of spectrum it has been necessary to assume that the linewidths of the individual lines are proportional to the M_i values to obtain the intensities of the outer lines relative to the center lines.

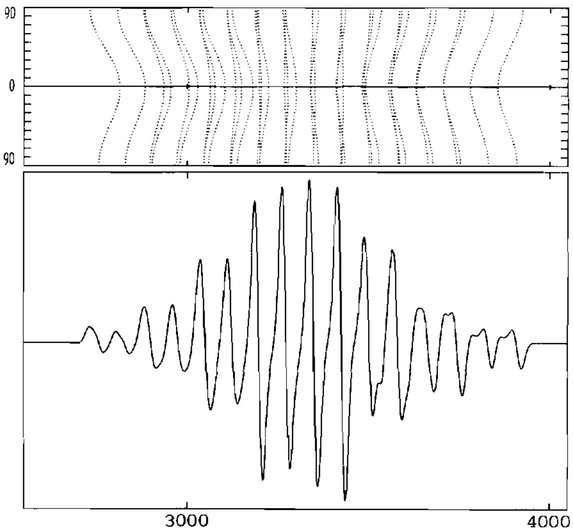

Fig. 5. The simulated EPR spectrum of complex **1a**. The upper curve gives the resonance condition as the magnetic field is rotated in the *xz* plane, while in the lower curve the magnetic field is rotated in the *yz* plane. The spectrum was calculated with the parameter values $A_{1x}=-0.0075$, $A_{1y}=-0.0072$, $A_{1z}=-0.0063$, $A_{2x}=-0.0073$, $A_{2y}=-0.0071$, $A_{2z}=-0.0068$ cm^{-1}; $g_{1x}=2.000$, $g_{1y}=1.998$, $g_{1z}=1.997$, $g_{2x}=g_{2y}=g_{2z}=1.994$.

Mn(IV,IV) complexes

Spectroscopy

The electronic spectrum of the Mn(IV,IV) complex is summarized in Table 5; the visible region of the spectrum is displayed in Fig. 6. The spectrum consists of two intense maxima in the UV region and two bands of medium intensity in the visible region. As has been observed in a variety of other Mn(IV,IV) complexes of this type [17], the broad maximum centered at 664 nm shows two low-energy shoulders at 710 and 780 nm.

Magnetic susceptibility

The temperature dependence of the magnetic susceptibility of a powdered sample of the (IV,IV) complex **2** was also measured in the range 2–300 K, and is presented in Fig. 7. For the Mn(IV,IV) complex, the effective magnetic moment is approximately 2.3 μ_B at room temperature and declines monotonically over the entire temperature range to a less than 0.5 μ_B. This behaviour is consistent with the expectation of a singlet ground state for the Mn(IV,IV) complex, and is also similar to that observed for other IV,IV complexes [17]. Presumably, the apparent decrease in the slope of the curve in Fig. 7 is due to the presence of some very small amount of paramagnetic material in the sample. Fitting of the magnetic data in the same manner as

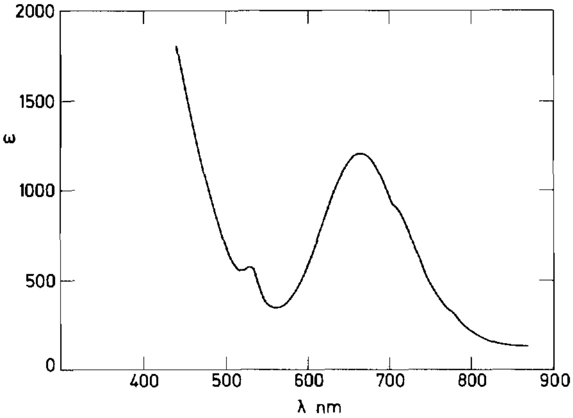

Fig. 6. The electronic absorption spectrum (visible region) of the Mn(IV,IV) complex **2** in 0.1 M perchloric acid. The intense band in the UV region at 390 nm is not shown so that the visible region is more clearly defined.

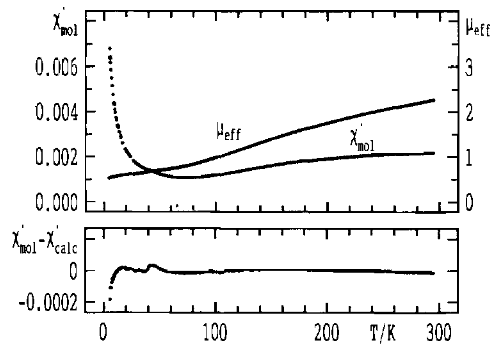

Fig. 7. The magnetic susceptibility (left scale) and effective magnetic moment (right scale) of the Mn(IV,IV) complex **2**. The lower curve shows the fit to the values calculated using the parameters $g_1=g_2=1.96$, $2J=-289$ cm^{-1}.

that used above for the Mn(III,IV) complexes leads to values of $g_1=g_2=1.96\pm0.01$, $2J=-289\pm2$ cm^{-1}, $J=-144.5\pm1$ cm^{-1}. This value of $2J$ is very similar to that of -288 cm^{-1} reported for the phen complex [2b], and is somewhat higher than those reported for other Mn(IV,IV) complexes of this type [6, 8, 14, 16].

Supplementary material

Table S1 (hydrogen atom parameters for **1a**), Table S2 (anisotropic thermal parameters for **1a**), and Table S3 (tabulation of observed and calculated structure amplitudes for **1a**) (20 pages) are available from D.J.H. on request.

Acknowledgements

We are grateful to Ms. Solveig Kallesøe for experimental assistance with the magnetic measurements. This work was supported by the National Science Foundation through grant No. CHE-9007607 (to D.J.H.), and by the Scientific Affairs Division, North Atlantic Treaty Organization (NATO) through grant No. CRG 910277 (to D.J.H., K.M. and J.G.).

References

1 (a)R. S. Nyholm and A. Turco, *Chem. Ind. (London)*, (1960) 74; (b) P. M. Plaksin, R. C. Stoufer, M. Mathew and G. J. Palenik, *J. Am. Chem. Soc., 94* (1972) 2121–2122.

2 (a) H. A. Goodwin and R. N. Sylva, *Aust. J. Chem., 20* (1967) 629–637; (b) M. Stebler, A. Ludi and H.-B. Bürgi, *Inorg. Chem., 25* (1986) 4743–4750.

3 M. A. Collins, D. J. Hodgson, K. Michelsen and E. Pedersen, *J. Chem. Soc., Chem. Commun.*, (1987) 1659–1660.

4 D. K. Towle, C. A. Botsford and D. J. Hodgson, *Inorg. Chim. Acta, 141* (1988) 167–168.

5 P. A. Goodson and D. J. Hodgson, *Inorg. Chem., 28* (1989) 3606–3608.

6 P. A. Goodson, J. Glerup, D. J. Hodgson, K. Michelsen and E. Pedersen, *Inorg. Chem., 29* (1990) 503–508.

7 P. A. Goodson, D. J. Hodgson and K. Michelsen, *Inorg. Chim. Acta, 172* (1990) 49–57.

8 A. R. Oki, J. Glerup and D. J. Hodgson, *Inorg. Chem., 29* (1990) 2435–2441.

9 P. A. Goodson, A. R. Oki, J. Glerup and D. J. Hodgson, *J. Am. Chem. Soc., 112* (1990) 6248–6254.

10 K. S. Hagen, W. H. Armstrong and H. Hope, *Inorg. Chem., 141* (1988) 167–168.

11 K. J. Brewer, A. Liegeois, J. W. Otvos, M. Calvin and L. O. Spreer, *J. Chem. Soc., Chem. Commun.*, (1988) 1219–1220.

12 M. Suzuki, H. Senda, Y. Kobayashi, H. Oshio and A. Uehara, *Chem. Lett.*, (1988) 1763–1766.

13 L. O. Spreer, personal communication; K. J. Brewer, M. Calvin, R. S. Lumpkin, J. W. Otvos and L. O. Spreer, *Inorg. Chem., 28* (1989) 4446–4451.

14 M. Suzuki, S. Tokura, M. Suhara and A. Uehara, *Chem. Lett.*, (1988) 477–480.

15 K. Wieghardt, U. Bossek, B. Nuber, J. Weiss, J. Bonvoisin, M. Corbella, S. E. Vitols and J. J. Girerd, *J. Am. Chem. Soc., 110* (1988) 7398–7411.

16 E. Libby, R. J. Webb, W. E. Streib, K. Folting, J. C. Huffman, D. N. Hendrickson and G. Christou, *Inorg. Chem., 28* (1989) 4037–4040.

17 P. A. Goodson, J. Glerup, D. J. Hodgson, K. Michelsen and H. Weihe, *Inorg. Chem., 30* (1991) 4909–4914.

18 D. J. Hodgson, E. Pedersen, H. Toftlund and C. Weiss, *Inorg. Chim. Acta, 120* (1986) 177–184.

19 P. A. Daugherty, J. Glerup, P. A. Goodson, D. J. Hodgson and K. Michelsen, *Acta Chem. Scand., 45* (1991) 244–253.

20 J. E. Richman and T. J. Atkins, *J. Am. Chem. Soc., 96* (1974) 2268–2270.

21 B. N. Figgis and R. S. Nyholm, *J. Chem. Soc.*, (1958) 4190.

22 J. Josephsen and E. Pedersen, *Inorg. Chem., 16* (1977) 2534–2538.

23 E. Pedersen, *Acta Chem. Scand., 26* (1972) 333–342.

24 G. M. Sheldrick, *SHELXTL-PLUS Crystallographic System*, Version 2, Nicolet XRD Corp., Madison, WI, 1987.

25 A. J. Bard and L. R. Faulkner, *Electrochemical Methods. Fundamentals and Applications*, Wiley, New York, 1980, Fig. E.1.

26 S. R. Cooper, G. C. Dismukes, M. P. Klein and M. Calvin, *J. Am. Chem. Soc., 100* (1978) 7248–7252.

27 V. H. Crawford, H. W. Richardson, J. R. Wasson, D. J. Hodgson and W. R. Hatfield, *Inorg. Chem., 15* (1976) 2107–2110.

28 J. Glerup, D. J. Hodgson and E. Pedersen, *Acta Chem. Scand., Ser. A, 37* (1983) 161–164.

29 E. Bang, J. Eriksen, J. Glerup, L. Mønsted, O. Mønsted and H. Weihe, *Acta Chem. Scand., 45* (1991) 367–372.

30 J. Glerup and H. Weihe, *Acta Chem. Scand., 45* (1991) 444–448.